Aging ballistic Lévy walks

Marcin Magdziarz* and Tomasz Zorawik
Faculty of Pure and Applied Mathematics, Hugo Steinhaus Center, Wroclaw University of Science and Technology, Wyspianskiego 27, 50-370 Wroclaw, Poland
(Received 21 December 2016; published 22 February 2017)

Aging can be observed for numerous physical systems. In such systems statistical properties [like probability distribution, mean square displacement (MSD), first-passage time] depend on a time span t_a between the initialization and the beginning of observations. In this paper we study aging properties of ballistic Lévy walks and two closely related jump models: wait-first and jump-first. We calculate explicitly their probability distributions and MSDs. It turns out that despite similarities these models react very differently to the delay t_a. Aging weakly affects the shape of probability density function and MSD of standard Lévy walks. For the jump models the shape of the probability density function is changed drastically. Moreover for the wait-first jump model we observe a different behavior of MSD when $t_a \ll t$ and $t_a \gg t$.

DOI: 10.1103/PhysRevE.95.022126

I. INTRODUCTION

Suppose we begin observations of a system which was initialized at $t = 0$ after some time t_a. There can be many reasons why we would want to do this, from technical restrictions of a measuring device to sheer curiosity. In many cases the delay largely changes statistical properties of the observed process. Such a phenomenon is called *aging*, a term which was originally used in the area of glassy materials [1–4]. Aging was also reported for blinking nanocrystals [5–8], where the changes between on and off state for a single, illuminated quantum dot during time interval $[t_a, t + t_a]$ were measured. It turned out that when the aging time t_a increases, more long on-state and off-state periods can be observed. Similar behavior is displayed by potassium channels dynamics [9]. For more examples see [10] and references therein.

In a recent paper [11] the authors studied statistical properties of aging continuous time random walks (CTRWs). In this article we develop a similar theory for a different, very useful model for anomalous diffusion—Lévy walk (LW). This model can be used, for instance, to describe the dynamics of the already mentioned blinking nanocrystals [5]. Other striking and sometimes very beautiful examples of applications include: migration of swarming bacteria [12], light transport in special optical materials (Lévy glass) [13], and foraging patterns of animals [14–16]. More examples are described in a review paper devoted to this model [17], see also [18]. The particle which perform Lévy walk moves with a constant velocity v (in this article for simplicity we set $v = 1$) for a time period which follows a power law $\psi(\tau) \propto \tau^{1+\alpha}$ with $\alpha > 0$. Then it chooses randomly a new direction of the motion [17]. Here we focus on the case $\alpha \in (0,1)$ which leads to a ballistic regime [19].

Lévy walks $L(t)$ can also be analyzed in a context of coupled continuous time random walks: the so-called wait-first $L_{WF}(t)$ and jump-first models $L_{JF}(t)$ [17]. The particle which performs wait-first Lévy walk instead of moving with the constant velocity v for time T remains motionless for time T and then executes a jump which length equals $v \cdot T$. As a result trajectories are discontinuous, contrary to the standard LW, see Fig. 1. The jump-first scenario differs from the wait-first case with the changed order of waiting and jumping moments. The CTRW approach to Lévy walks was analyzed in Refs. [20,21]. Although the jump models and the standard Lévy walk appear to be very similar, they have very different statistical properties. In Ref. [19] a method to find probability density functions $p(x,t)$ (PDFs) for all these models in the ballistic regime was proposed by Froemberg *et al.* For another approach to this problem for the jump models see [22]. It is also worth to mention that PDFs of multidimensional isotropic Lévy walks were found in Refs. [23,24]. We emphasize that all the results we present here are calculated for the diffusion limits of LW and two other coupled CTRW models [25,26].

In what follows we assume aging time $t_a > 0$ and analyze aging Lévy walk $X_a(t)$, wait-first $Y_a(t)$, and jump-first $Z_a(t)$ models, where

$$\begin{aligned} X_a(t) &= L(t + t_a) - L(t_a), \\ Y_a(t) &= L_{WF}(t + t_a) - L_{WF}(t_a), \\ Z_a(t) &= L_{JF}(t + t_a) - L_{JF}(t_a). \end{aligned} \tag{1}$$

We propose a method to compute distributions $p(dx, t_a, t)$ of aging LWs and calculate ensemble and time averaged MSDs. One should underline here that the distribution function of the time averaged intensity correlation function for standard LWs was computed in Ref. [5].

II. AGING CONTINUOUS LÉVY WALKS

In this section we calculate the distribution $p(dx, t_a, t)$ of aging Lévy walk $X_a(t)$. The forward renewal time W_{t_a} after t_a for the non-aging process $L(t)$ has the distribution [11,27–30]

$$f(t_a, w) = \frac{\sin(\pi\alpha)}{\pi} \frac{t_a^{\alpha}}{w^{a}(t_a + w)} \mathbf{1}_{0 \leqslant w}, \tag{2}$$

where $\mathbf{1}_{A(w)}$ denotes the indicator function which equals 1 when $A(w)$ is true and 0 otherwise. This issue can be also

*Corresponding author: marcin.magdziarz@pwr.edu.pl

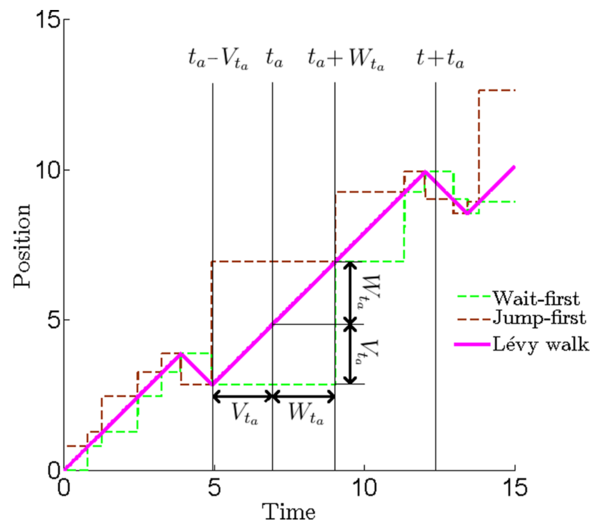

FIG. 1. Sample trajectories of Lévy walks. Forward renewal time - W_{t_a}, backward renewal time - V_{t_a}.

studied in the language of stable subordinators [31]. Now, at the moment of the renewal the process $L(t)$ is time-homogeneous and Markovian [32] so $L(t+t_a) - L(t_a + W_{t_a})$ has the same distribution as $L(t - W_{t_a})$ on the set $\{\omega \in \Omega : W_{t_a}(\omega) \leqslant t\}$. Moreover $L(t+t_a) - L(t_a + W_{t_a})$ is independent from W_{t_a} and $L(t_a + W_{t_a})$. We also notice that at the moment t_a the particle can be moving upward and downward with the same probability. In the first case at the moment $t_a + W_{t_a}$ the particle is located at $L(t_a) + W_{t_a}$ and

$$L(t+t_a) - L(t_a) = L(t+t_a) - L(t_a + W_{t_a}) + W_{t_a},$$

whereas in the second case at $L(t) + W_{t_a}$ and

$$L(t+t_a) - L(t_a) = L(t+t_a) - L(t_a + W_{t_a}) - W_{t_a},$$

see Fig. 1. Therefore

$$\begin{aligned} p\big(dx,t_a,t,W_{t_a} \leqslant t\big) &= \int_{w=0}^{t} f(t_a,w)\frac{\phi_{t-w}(x-w)+\phi_{t-w}(x+w)}{2}dwdx \\ &= \frac{\sin(\pi\alpha)t_a^{\alpha}}{2\pi}\int_{w=0}^{t}\frac{\phi_{t-w}(x-w)+\phi_{t-w}(x+w)}{w^{\alpha}(w+t_a)}dwdx, \end{aligned} \tag{3}$$

where

$$\phi_t(y) = \frac{\sin(\pi\alpha)}{\pi}\frac{(t-y)^{\alpha}(t+y)^{\alpha-1}+(t+y)^{\alpha}(t-y)^{\alpha-1}}{(t-y)^{2\alpha}+(t+y)^{2\alpha}+2\cos(\pi\alpha)(t^2-y^2)^{\alpha}}\mathbf{1}_{|y|<t} \tag{4}$$

is a PDF of non-aging Lévy walk [19]—Lamperti distribution [33]. If there is no renewal between t_a and $t+t_a$ we have

$$p\big(dx,t_a,t,W_{t_a} > t\big) = \int_t^{\infty} f(t_a,w)dw\left(\frac{\delta_{-t}(dx)+\delta_t(dx)}{2}\right) = \frac{\sin(\pi\alpha)}{2\alpha\pi}\left(\frac{t_a}{t}\right)^{\alpha} {}_2F_1\left[1,\alpha,1+\alpha,-\frac{t_a}{t}\right](\delta_{-t}(dx)+\delta_t(dx)). \tag{5}$$

Adding $p(dx,t_a,t,W_{t_a} \leqslant t)$ and $p(dx,t_a,t,W_{t_a} > t)$ yields

$$\begin{aligned} p(dx,t_a,t) &= \frac{\sin(\pi\alpha)}{2\alpha\pi}\left(\frac{t_a}{t}\right)^{\alpha} {}_2F_1\left[1,\alpha,1+\alpha,-\frac{t_a}{t}\right](\delta_{-t}(dx)+\delta_t(dx)) \\ &\quad + \frac{\sin(\pi\alpha)t_a^{\alpha}}{2\pi}\int_{w=0}^{t}\frac{\phi_{t-w}(x-w)+\phi_{t-w}(x+w)}{w^{\alpha}(w+t_a)}dwdx\mathbf{1}_{|x|<t}, \end{aligned} \tag{6}$$

where $\phi_t(r)$ is given by Eq. (4). The PDF of the aging Lévy walk has a similar shape to the standard Lévy walk—see Fig. 2. However now the distribution has additionally two δ peaks at $x = t$ and $x = -t$ which correspond to the probability that the particle moves straight in one direction for the whole time period $(0,t)$. In the special case $\alpha = 0.5$ the distribution $p(dx,t_a,t)$ can be written in a simpler form:

$$p(dx,t_a,t) = \frac{1}{\pi}\arctan\left(\sqrt{\frac{t_a}{t}}\right)(\delta_{-t}(dx)+\delta_t(dx)) + \frac{1}{2\pi}\left(\frac{1}{\sqrt{(t+2t_a+x)(t-x)}} + \frac{1}{\sqrt{(t+2t_a-x)(t+x)}}\right)\mathbf{1}_{|x|<t}dx. \tag{7}$$

We notice that when $t_a \to 0$ (no aging), the δ peaks disappear and the PDF tends to the PDF of the non-aging Lévy walk.

We also compared the analytical results with the densities estimated via Monte Carlo methods. It turns out (see Fig. 2) that the theory and simulations match very well. The algorithm to simulate trajectories of non-aging Lévy walks $X(t)$ was presented in Refs. [23,34]. To adjust it for aging Lévy walks $X_{t_a}(t)$ we used their definition given by Eq. (1). A similar approach can be applied for the modifications of Lévy walks, as discussed in the next sections.

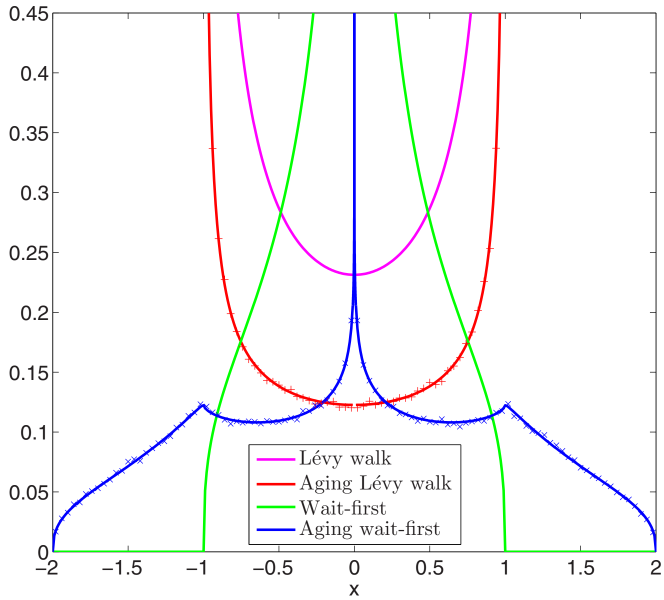

FIG. 2. Lines—PDFs of different Lévy walks, $t_a = 1, t = 1$, and $\alpha = 0.4$. Pluses and crosses—PDFs estimated using Monte Carlo methods from 10^6 trajectories of LW and wait-first LW, respectively.

A. Ensemble average

Knowing the distribution $p(dx,t_a,t)$ we can calculate immediately an ensemble averaged mean square displacement for the aging Lévy walk for all $\alpha \in (0,1)$:

$$\begin{aligned}\langle X_a^2(t)\rangle &= \int_{\mathbb{R}} x^2 p(dx,t_a,t)\\ &= t_a^2 + (1-\alpha)(t+t_a)^2\\ &\quad - \frac{\sin(\pi\alpha)}{\pi(1-\alpha)} t_a^\alpha t^{1-\alpha}(t_a + (1-a)(t_a+t))\\ &\quad + \frac{\sin(\pi\alpha)}{\alpha\pi}(t+t_a)t_a^\alpha t^{-\alpha}(\alpha(t+t_a)-2t_a)\\ &\quad \times {}_2F_1\left[1,\alpha,1+\alpha,-\frac{t_a}{t}\right]. \end{aligned} \tag{8}$$

One can also deduce this form of MSD from [35] where the correlation function was computed. It can be shown that the mean square displacement has the following asymptotics:

$$\langle X_a^2(t)\rangle \approx \begin{cases} t^2, & t \ll t_a\\ (1-\alpha)t^2, & t \gg t_a \end{cases}. \tag{9}$$

Indeed, when $t \gg t_a$, this can be easily read from Eq. (8). We recover the result for ensemble averaged MSD of non-aging Lévy walk [35–37]. In the opposite case we apply the identities for the hypergeometric functions [38] and obtain

$$\begin{aligned}\langle X_a^2(t)\rangle &= t^2 - \frac{\sin(\pi\alpha)}{\pi(1-\alpha)} {}_2F_1\left[1,\alpha,1+\alpha,-\frac{t}{t_a}\right]\left(\frac{t}{t_a}\right)^{1-a}\\ &\quad \times \big((2-\alpha)t_a^2 + (1-a)tt_a\\ &\quad + (t+t_a)((\alpha-2)t_a + \alpha t)\big). \end{aligned} \tag{10}$$

Now we take into account the asymptotic behavior for ${}_2F_1[1,\alpha,1+\alpha,z]$ when $|z| \to 0$ and Eq. (9) follows. As we can see, the aging has a weak effect on MSD behavior—it only changes the constant. Recall that for the aging CTRW the situation was different—a regime change was observed [29]:

$$\langle x_a^2(t)\rangle \approx \begin{cases} t t_a^{\alpha-1}/\Gamma(\alpha), & t \ll t_a\\ t^\alpha/\Gamma(1+\alpha), & t \gg t_a \end{cases}. \tag{11}$$

B. Time average

We can also calculate an expected value of a time averaged MSD for aging Lévy walks

$$\begin{aligned}&\langle\overline{\delta^2(\Delta,t_a,T)}\rangle\\ &= \left\langle \frac{1}{T-\Delta}\int_{t_a}^{t_a+T-\Delta}(X(t'+\Delta)-X(t'))^2 dt'\right\rangle\\ &= \frac{1}{T-\Delta}\int_{t_a}^{t_a+T-\Delta}\langle X_{t'}^2(\Delta)\rangle dt', \end{aligned} \tag{12}$$

where $\langle X_{t'}^2(\Delta)\rangle$ is given by Eq. (8). In a highly aged regime $t_a \gg T \gg \Delta$ we obtain an equivalence between time and ensemble average

$$\langle\overline{\delta^2(\Delta,t_a,T)}\rangle \sim \Delta^2 \sim \langle X_a^2(\Delta)\rangle. \tag{13}$$

A very similar phenomena was also observed for aging CTRWs [11].

III. AGING WAIT-FIRST LÉVY WALKS

For aging wait-first model $Y_a(t)$ the situation is different. Let W_{t_a} be the forward renewal time after t_a for the non-aging process $Y(t)$. To calculate distribution $p(dx,t_a,t)$ of $Y_a(t)$ we cannot repeat the same reasoning as for aging Lévy walks. The position of the particle at the moment $t_a + W_{t_a}$ is unknown, even if we know the value of W_{t_a}. At this moment the particle performs a jump, but the length of this jump depends on how long the particle was resting. We have to include in our equation V_{t_a}—the backward renewal time. Then the particle at time $t_a + W_{t_a}$ is located at $L_{WF}(t_a) \pm (W_{t_a} + V_{t_a})$ with equal probability—jumping up and down is equally probable. The joint distribution of a random vector (V_{t_a}, W_{t_a}) can be computed from Theorem 2.3 in Ref. [32]:

$$f(t_a,v,w) = \frac{\alpha\sin(\pi\alpha)}{\pi}\frac{1}{(w+v)^{1+\alpha}(t_a-v)^{1-\alpha}}\mathbf{1}_{0\leqslant v\leqslant t_a}\mathbf{1}_{0\leqslant w}. \tag{14}$$

Therefore, in case there is a renewal between t and t_a we get

$$\begin{aligned}p\big(dx,t_a,t,W_{t_a}\leqslant t\big) &= \frac{\alpha\sin(\pi\alpha)}{2\pi}\int_{v=0}^{t_a}\int_{w=0}^{t}\\ &\quad \times \frac{\phi_{t-w}(x-v-w)+\phi_{t-w}(x+v+w)}{(w+v)^{1+\alpha}(t_a-v)^{1-a}}\\ &\quad \times dv\,dw\,dx\,\mathbf{1}_{|x|<t+t_a}, \end{aligned} \tag{15}$$

where

$$\begin{aligned}\phi_t(r) &= \frac{2\sin(\pi\alpha)}{\pi}\\ &\quad \times \frac{|r|^{\alpha-1}(t-|r|)^\alpha}{(t+r)^{2\alpha}+(t-r)^{2\alpha}+2\cos(\pi\alpha)(t^2-r^2)^\alpha}\mathbf{1}_{|r|<t} \end{aligned} \tag{16}$$

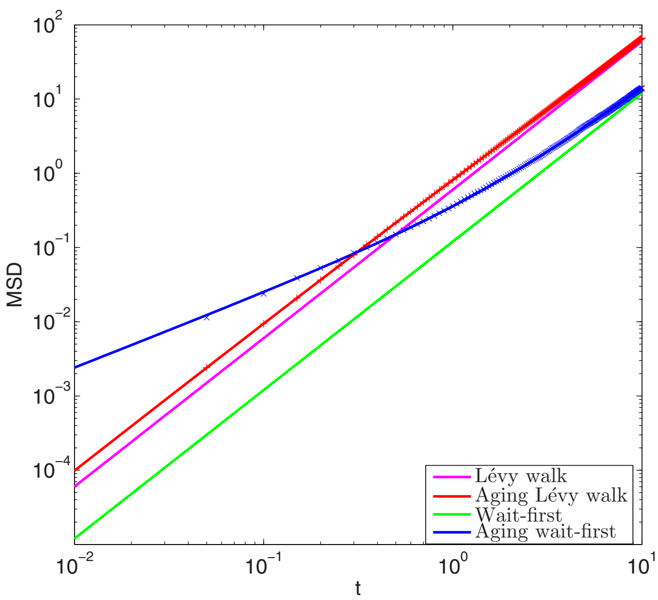

FIG. 3. Lines—ensemble averaged MSD (t_a,t), $t_a = 1$, and $\alpha = 0.4$. Pluses and crosses—ensemble averaged MSDs estimated using Monte Carlo methods from 10^4 trajectories of LW and wait-first model, respectively.

is a PDF of non-aging wait-first model. In case $W_{t_a} > t$ the particle remains in the same position, that is $Y_a(t) = Y_a(0)$ and

$$p\big(dx,t_a,t,W_{t_a} > t\big) = \frac{\sin(\pi\alpha)}{\alpha\pi}\left(\frac{t_a}{t}\right)^{\alpha} {}_2F_1\left[1,\alpha,1+\alpha,-\frac{t_a}{t}\right]\delta_0(dx). \quad (17)$$

Adding Eqs. (15) and (17) we obtain

$$\begin{aligned} p(dx,t_a,t) &= \frac{\sin(\pi\alpha)}{\alpha\pi}\left(\frac{t_a}{t}\right)^{\alpha} {}_2F_1\left[1,\alpha,1+\alpha,-\frac{t_a}{t}\right]\delta_0(dx) \\ &\quad + \frac{\alpha\sin(\pi\alpha)}{2\pi}\int_{v=0}^{t_a}\int_{w=0}^{t} \\ &\quad \times \frac{\phi_{t-w}(x-v-w)+\phi_{t-w}(x+v+w)}{(w+v)^{1+\alpha}(t_a-v)^{1-a}} \\ &\quad \times dv\,dw\,dx\,\mathbf{1}_{|x|<t+t_a}, \end{aligned} \quad (18)$$

where $\phi_t(r)$ is given by Eq. (16). The density of aging wait-first model is supported on $(-t_a - t, t_a + t)$, whereas the density of aging LW on $(-t,t)$—Fig. 2. This is connected with the fact, that for wait-first model, when we start our observations, the particle could be resting for a very long time close to t_a and then it can perform a long jump (up to $t_a + t$). In other words $|Y_a(t)| \leqslant t + t_a$, whereas for a non-aging process we have $|Y(t)| \leqslant t$.

A. Ensemble average

We now turn to the ensemble average of the aging wait-first model $Y_a(t)$. After using the formula for the distribution $p(dx,t_a,t)$ we get

$$\langle Y_a^2(t)\rangle = \int_{\mathbb{R}} x^2 p(dx,t_a,t) = \frac{\alpha(1-\alpha)}{2}\big((t+t_a)^2 - t_a^2\big). \quad (19)$$

Consequently,

$$\langle Y_a^2(t)\rangle \approx \begin{cases} \alpha(1-\alpha)t_a t, & t_a \gg t \\ \frac{\alpha(1-\alpha)}{2}t^2, & t_a \ll t \end{cases}. \quad (20)$$

We observe a completely different behavior of MSD in slightly and highly aged systems. It is curious that for standard aging Lévy walks this was not the case—the result was the same up to a multiplication by the constant [Eq. (9)], see Fig. 3. The difference can be explained in the following way. If we start our observations at t_a, then the initial waiting time is significantly shorter than the next jump, so the displacement is bigger compared to the standard model without aging. This fact implies that the MSD for the aging particle is linear for short times. When $t_a \ll t$ this phenomenon has little effect on the position of the particle at time $t_a + t$ and we recover the ballistic regime. On the other hand if the particle moves according to the standard Lévy walk, the velocity of the particle is always constant. If we start our observation at t_a only a distribution of subsequent turns is changed compared to the non-aging system. Thus the ballistic regime holds for aging Lévy walk both for short and long times.

B. Time average

Similarly as in the case of the aging standard LW, we calculate the time average of the aging wait-first model

$$\begin{aligned} \langle\overline{\delta^2(\Delta,t_a,T)}\rangle &= \left\langle \frac{1}{T-\Delta}\int_{t_a}^{t_a+T-\Delta}(Y(t'+\Delta)-Y(t'))^2dt'\right\rangle \\ &= \frac{1}{T-\Delta}\int_{t_a}^{t_a+T-\Delta}\langle Y_{t'}^2(\Delta)\rangle dt' \\ &= \frac{\alpha(1-\alpha)}{2}(T+2t_a)\Delta. \end{aligned} \quad (21)$$

Although the behavior of the time-averaged MSD for the standard and wait-first model is different, in this case we also observe that in a highly aged system ($t_a \gg T$) we have the following equivalence (analogous to Eq. (13) and the result for aging CTRWs from [11]):

$$\langle\overline{\delta^2(\Delta,t_a,T)}\rangle \sim \alpha(1-\alpha)t_a\Delta \sim \langle Y_a^2(\Delta)\rangle. \quad (22)$$

IV. AGING JUMP-FIRST LÉVY WALKS

The case of aging jump-first model $Z_a(t)$ is a little bit similar to the aging LWs. Once again we set W_{t_a} to be the forward renewal time after t_a for the non-aging jump-first model $Z(t)$. We do not need the backward renewal time. At time point $t_a + W_{t_a}$ the particle ends its waiting period so $Z((t_a + W_{t_a})^-) = Z(t_a)$, which distinguishes the jump-first model from the LW. Further movement $Z(t_a + W_{t_a} + t) - Z((t_a + W_{t_a})^-)$ is independent from the position $Z((t_a + W_{t_a})^-)$ and W_{t_a}. Thus

$$\begin{aligned} p(dx,t_a,t) &= \frac{\sin(\pi\alpha)}{\alpha\pi}\left(\frac{t_a}{t}\right)^{\alpha} {}_2F_1\left[1,\alpha,1+\alpha,-\frac{t_a}{t}\right]\delta_0(dx) \\ &\quad + \frac{\sin(\pi\alpha)t_a^{\alpha}}{\pi}\int_{w=0}^{t}\frac{\phi_{t-w}(x)}{w^{\alpha}(w+t_a)}dw\,dx, \end{aligned} \quad (23)$$

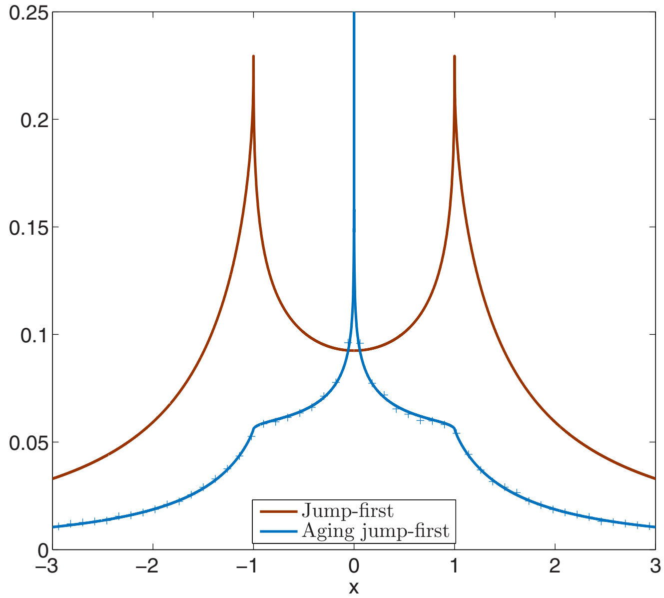

FIG. 4. Lines—densities of aging $Z_{t_a}(1)$ and non-aging $Z(1)$ jump-first models. Aging time $t_a = 1$, $\alpha = 0.4$. Pluses—the density estimated using MC methods from 10^6 trajectories.

where

$$\phi_t(r) = \frac{\sin(\pi\alpha)}{\pi}\frac{t^\alpha}{r}\begin{cases} \frac{\operatorname{sign} r}{|r+t|^\alpha+|r-t|^\alpha} & t \leqslant |r| \\ \frac{|r+t|^\alpha-|r-t|^\alpha}{|r+t|^{2\alpha}+|r-t|^{2\alpha}+2\cos(\pi\alpha)|r^2-t^2|^\alpha} & t > |r| \end{cases}. \tag{24}$$

Figure 4 shows the density of the absolutely continuous part of the distribution $p(dx,t_a,t)$. We observe that the aging changes the shape of the PDF. Two sharp peaks at $x = t$ and $x = -t$ characteristic for the non-aging process disappear and a singularity at $x = 0$ emerges.

We do not study the effect of aging for the time and ensemble averaged MSDs since for this process both are infinite. This can be deduced by analyzing the absolutely continuous part of $p(dx,t_a,t)$ when $x \to \infty$. We have $\phi_t(r) \approx c_1 t^\alpha r^{-1-\alpha}$ when $r \gg t$, where c_1 is a constant. Therefore from Eq. (23) we obtain that for set t_a and t the continuous part of $p(dx,t_a,t)$ has the asymptotics $p(dx,t_a,t) \propto c_2 x^{-1-\alpha} dx$ when $x \to \infty$, where c_2 is a constant which depends on t_a and t. Since $\alpha \in (0,1)$ the MSD is infinite. The non-aging jump-first model has the same property (see [19]).

V. CONCLUSIONS

We considered three different anomalous diffusion models in the context of aging. We computed their distributions $p(dx,t_a,t)$ and used them for finding time and ensemble averaged MSDs. It turns out that the delay between the initialization of the system and the beginning of the observations affects those models in different way: the standard Lévy walks appear to be the least prone to aging. It is an open problem if it is possible to apply the methods from this paper to other velocity models of Lévy walks [19,39].

ACKNOWLEDGMENT

This research was partially supported by NCN Maestro grant no. 2012/06/A/ST1/00258.

[1] E. M. Bertin and J. P. Bouchaud, Phys. Rev. E **67**, 026128 (2003).
[2] C. Monthus and J.-P. Bouchaud, J. Phys. A **29**, 3847 (1996).
[3] L. C. E. Struik, Polym. Eng. Sci. **17**, 165 (1977).
[4] S. Burov and E. Barkai, Phys. Rev. Lett. **98**, 250601 (2007).
[5] G. Margolin and E. Barkai, Phys. Rev. Lett. **94**, 080601 (2005).
[6] G. Margolin and E. Barkai, J. Chem. Phys. **121**, 1566 (2004).
[7] F. D. Stefani, J. P. Hoogenboom, and E. Barkai, Phys. Today **62**, 34 (2009).
[8] X. Brokmann, J.-P. Hermier, G. Messin, P. Desbiolles, J.-P. Bouchaud, and M. Dahan, Phys. Rev. Lett. **90**, 120601 (2003).
[9] A. V. Weigel, B. Simon, M. M. Tamkun, and D. Krapf, Proc. Natl. Acad. Sci. USA **108**, 6438 (2011).
[10] R. Metzler, J. H. Jeon, A. G. Cherstvy, and E. Barkai, Phys. Chem. Chem. Phys. **16**, 24128 (2014).
[11] J. H. P. Schulz, E. Barkai, and R. Metzler, Phys. Rev. X **4**, 011028 (2014).
[12] G. Ariel, A. Rabani, S. Benisty, J. D. Partridge, R. M. Harshey, and A. Be'er, Nature Communications **6**, 8396 (2015).
[13] P. Barthelemy, P. J. Bertolotti, and D. S. Wiersma, Nature **453**, 495 (2008).
[14] W. J. Bell, *Searching Behaviour: The Behavioural Ecology of Finding Resources* (Chapman and Hall, London, 1991).
[15] H. C. Berg, *Random Walks in Biology* (Princeton University Press, Princeton, 1993).
[16] M. Buchanan, Nature **453**, 714 (2008).
[17] V. Zaburdaev, S. Denisov, and J. Klafter, Rev. Mod. Phys. **87**, 483 (2015).
[18] J. Klafter and I. M. Sokolov, *First Steps in Random Walks. From Tools to Applications* (Oxford University Press, Oxford, 2011).
[19] D. Froemberg, M. Schmiedeberg, E. Barkai, and V. Zaburdaev, Phys. Rev. E **91**, 022131 (2015).
[20] M. F. Shlesinger, J. Klafter, and Y. M. Wong, J. Stat. Phys. **27**, 499 (1982).
[21] J. Klafter, A. Blumen, and M. F. Shlesinger, Phys. Rev. A **35**, 3081 (1987).
[22] M. Magdziarz and T. Zorawik, Frac. Calc. Appl. Anal. **19**, 1488 (2016).
[23] M. Magdziarz and T. Zorawik, Phys. Rev. E **94**, 022130 (2016).
[24] M. Magdziarz and T. Zorawik, Commun. Nonlinear Sci. Numer. Simul. **48**, 462 (2017).
[25] M. Magdziarz and M. Teuerle, Commun. Nonlinear Sci. Numer. Simul. **20**, 489 (2015).
[26] M. Magdziarz, H. P. Scheffler, P. Straka, and P. Zebrowski, Stoch. Proc. Appl. **125**, 4021 (2015).

[27] J. H. P. Schulz, E. Barkai, and R. Metzler, Phys. Rev. Lett. **110**, 020602 (2013).

[28] E. Barkai, Phys. Rev. Lett. **90**, 104101 (2003).

[29] E. Barkai and Y. C. Cheng, J. Chem. Phys. **118**, 6167 (2003).

[30] C. Godrèche and J. M. Luck, J. Stat. Phys. **104**, 489 (2001).

[31] J. Bertoin, in *Subordinators: Examples and Applications*, in Lectures on Probability Theory and Statistics, edited by P. Bernard (Berlin, Springer, 2000).

[32] M. M. Meerschaert and P. Straka, Ann. Probab. **42**, 1699 (2014).

[33] J. Lamperti, Trans. Amer. Math. Soc. **88**, 380 (1958).

[34] M. Magdziarz, W. Szczotka, and P. Żebrowski, J. Stat. Phys. **147**, 74 (2012).

[35] D. Froemberg and E. Barkai, Phys. Rev. E **87**, 030104(R) (2013).

[36] D. Froemberg and E. Barkai, Phys. Rev. E **88**, 024101 (2013).

[37] D. Froemberg and E. Barkai, Eur. Phys. J. B **86**, 331 (2013).

[38] M. Abramowitz and I. A. Stegun, *Hypergeometric Functions*, Chap. 15 in Handbook of Mathematical Functions with Formulas, Graphs, and Mathematical Tables (Dover, New York, 1972), pp. 555–566.

[39] A. Rebenshtok and E. Barkai, J. Stat. Phys. **133**, 565 (2008).